Han et al. *Zool. Res.* 2021, 42(5): 548−561
https://doi.org/10.24272/j.issn.2095-8137.2021.116

ZR | Zoological Research

Article Open Access

Whole-genome resequencing of Japanese whiting (*Sillago japonica*) provide insights into local adaptations

Zhi-Qiang Han[1], Xin-Yu Guo[2], Qun Liu[2], Shan-Shan Liu[2], Zhi-Xin Zhang[3], Shi-Jun Xiao[4,*], Tian-Xiang Gao[1,*]

[1] *Fishery College*, *Zhejiang Ocean University*, *Zhoushan*, *Zhejiang* 316002, *China*

[2] *BGI-Qingdao*, *BGI-Shenzhen*, *Qingdao*, *Shandong* 266555, *China*

[3] *Graduate School of Marine Science and Technology*, *Tokyo University of Marine Science and Technology*, *Konan*, *Minato*, *Tokyo* 108-8477, *Japan*

[4] *Institute of Fisheries Science*, *Tibet Academy of Agricultural and Animal Husbandry Sciences*, *Lhasa*, *Tibet* 850000, *China*

ABSTRACT

The genetic adaptations of various organisms to heterogeneous environments in the northwestern Pacific remain poorly understood. Heterogeneous genomic divergence among populations may reflect environmental selection. Advancing our understanding of the mechanisms by which organisms adapt to different temperatures in response to climate change and predicting the adaptive potential and ecological consequences of anthropogenic global warming are critical. We sequenced the whole genomes of Japanese whiting (*Sillago japonica*) specimens collected from different latitudinal locations along the coastal waters of China and Japan to detect possible thermal adaptations. Using population genomics, a total of 5.48 million single nucleotide polymorphisms (SNPs) from five populations revealed a complete genetic break between the Chinese and Japanese groups, which was attributed to both geographic distance and local adaptation. The shared natural selection genes between two isolated populations (i.e., Zhoushan and Ise Bay/Tokyo Bay) indicated possible parallel evolution at the genetic level induced by temperature. These genes also indicated that the process of temperature selection on isolated populations is repeatable. Moreover, we observed natural candidate genes related to membrane fluidity, possibly underlying adaptation to cold environmental stress. These findings advance our understanding of the genetic mechanisms underlying the rapid adaptations of fish species. Species distribution projection models suggested that the Chinese and Japanese groups may have different responses to future climate change, with the former expanding and the latter contracting. The findings of this study enhance our understanding of genetic differentiation and adaptation to changing environments.

Keywords: *Sillago japonica*; Local adaptation; Climate change; Temperature stress; Whole-genome resequencing

INTRODUCTION

A fundamental question in biology is how organisms adapt to

Received: 06 April 2021; Accepted: 28 July 2021; Online: 29 July 2021
Foundation items: The study was supported by the National Natural Science Foundation of China (41976083, 41776171 and 32072980)
*Corresponding authors, E-mail: shijun_xiao@163.com; gaotianxiang0611@163.com

diverse and changing environments (Schluter & McPeek, 2000). Spatially varying selection usually triggers differential adaptations of local populations and ultimately initiates evolutionary diversification and speciation (Ferchaud & Hansen, 2016; Fustier et al., 2017). Identification of the genetic basis for ecological adaptation is not only a primary goal of evolutionary biology but is also required to define conservation units for management (Balanyà et al., 2009; Chen et al., 2018a; Skelly et al., 2007). Moreover, detecting candidate genes under natural selection could help identify key gene pathways involved in adaptations to local environments. The marine environment is undergoing marked changes, most especially rising temperature, which is a major environmental factor that influences spatial distribution and diversity of fish species (Chen et al., 2018b). Advancing our understanding of thermal adaptation is critical in predicting the adaptive potential and ecological consequences of anthropogenic global warming.

Global climate change has considerable effects on organisms, especially coastal species. The influence of climate change on marine organisms is intensified in the East China and Yellow seas, where water is warming at a higher rate than in other areas (Cai et al., 2020). Simulation results have indicated that even under the low greenhouse emission scenario (i.e., RCP4.5), the average annual sea surface temperature in the Yellow Sea will increase by at least 2 °C by the end of the 21st century (http://www.bio-oracle.org/) (Assis et al., 2018). Therefore, climate-mediated selection signatures must be detected. Restriction site-associated DNA tag sequencing (RAD-seq) and genotyping-by-sequencing (GBS) have been applied in investigations on the genetic adaptations of organisms in the northwestern Pacific. However, these methods only cover a fraction of the total genome and may miss numerous loci under selection in local adaptations (Li et al., 2019; Wang et al., 2016; Xu et al., 2017). Furthermore, studies on population genomics conducted in this region have only revealed a possible signature of thermal adaptation, and no population-specific genomic regions or genes related to warm or cold temperature stress have been analyzed. Adaptations to high or low temperatures are expected to have highly polygenic backgrounds, which are difficult to detect using reduced representation genome sequencing. In addition to possible local adaptations, the similar distribution of ocean surface temperature between the coastal waters of China and Japan may lead to identical or similar adaptive changes in distantly independent populations, thereby causing parallel evolution.

Recent population-scale genomic study of Japanese whiting (*Sillago japonica*; Family Sillaginidae) suggested that it may be an ideal model for detecting signatures of parallel selection (Yang et al., 2020). This fish is a commercially important coastal species widely distributed throughout the northwestern Pacific, especially the East China Sea, Yellow Sea, and coastal waters of Japan (McKay, 1992; Oozeki et al., 1992). This species is euryhaline but does not migrate over long distances (Yang et al., 2020). GBS markers indicate that there are substantial genetic differences between the Chinese and Japanese populations, with the Rushan (RS) (Weihai City, China) population considered a transitional population between China and Japan (Yang et al., 2020), indicating that the species has dispersed from the South China Sea to the East China Sea, Yellow Sea, and coastal waters of Japan. These findings support the supposition that the *S. japonica* populations in the East China Sea and coastal waters of Japan are independent genetic populations. The Yellow Sea population, which dispersed from the East China Sea, may tolerate cold temperature stress during winter and may exhibit genomic adaptations to such temperatures. The Japanese population, which originated from the Yellow Sea, may suffer warm temperature stress. Although the East China Sea populations from western coastal China originated from the South China Sea, these populations and some Japanese populations encounter similar temperature stress, which could cause parallel evolution and natural selection on identical genes. Therefore, *S. japonica* is an interesting species for studies on ecological adaptation because it inhabits diverse environments, ranging from tropical to warm temperate climates, and it shows low levels of genetic differentiation at neutral loci (Gao et al., 2019; Kashiwagi et al., 2000). A draft *S. japonica* genome was previously sequenced by the BGI-Shenzhen Company, China (unpublished data). This draft genome provides a fundamental resource for whole-genome resequencing and population genomic research.

In the present study, we sequenced the whole genomes of 49 *S. japonica* individuals collected from five sites across the coastal waters of China and Japan, covering high-temperature (mean annual temperature >25 ℃), warm-temperature (mean annual temperature >19 ℃), and cold-temperature (mean annual temperature >14 ℃) areas. This study provides insights into the evolutionary history and genetic diversity of *S. japonica*, as well as the mechanisms by which a species can adapt to different thermal environments, especially cold regions. By comparing genomes from low- and high-temperature environments, we identified several candidate genes with potential molecular functions in local temperature adaptations among the *S. japonica* populations inhabiting different thermal environments. Comparison of *S. japonica* populations from the East China Sea and coastal waters of Japan may provide evidence of parallel evolution within this species.

MATERIALS AND METHODS

Sampling

We collected 49 individuals of *S. japonica* from five populations distributed throughout the coastal waters of China and Japan (Figure 1; Table 1). All individuals were identified based on morphological features. A piece of muscle tissue was obtained from each individual and preserved in 95% ethanol or frozen for DNA extraction.

Sequencing, read mapping, and single nucleotide polymorphism (SNP) calling

Genome sequencing was performed using the Illumina HiSeq 2500 platform by Novogene Bioinformatics Technology Co., Ltd., China. Raw read quality control and removal of potential adaptor sequences were performed to ensure the accuracy of bioinformatics analysis. Paired-end reads from each individual

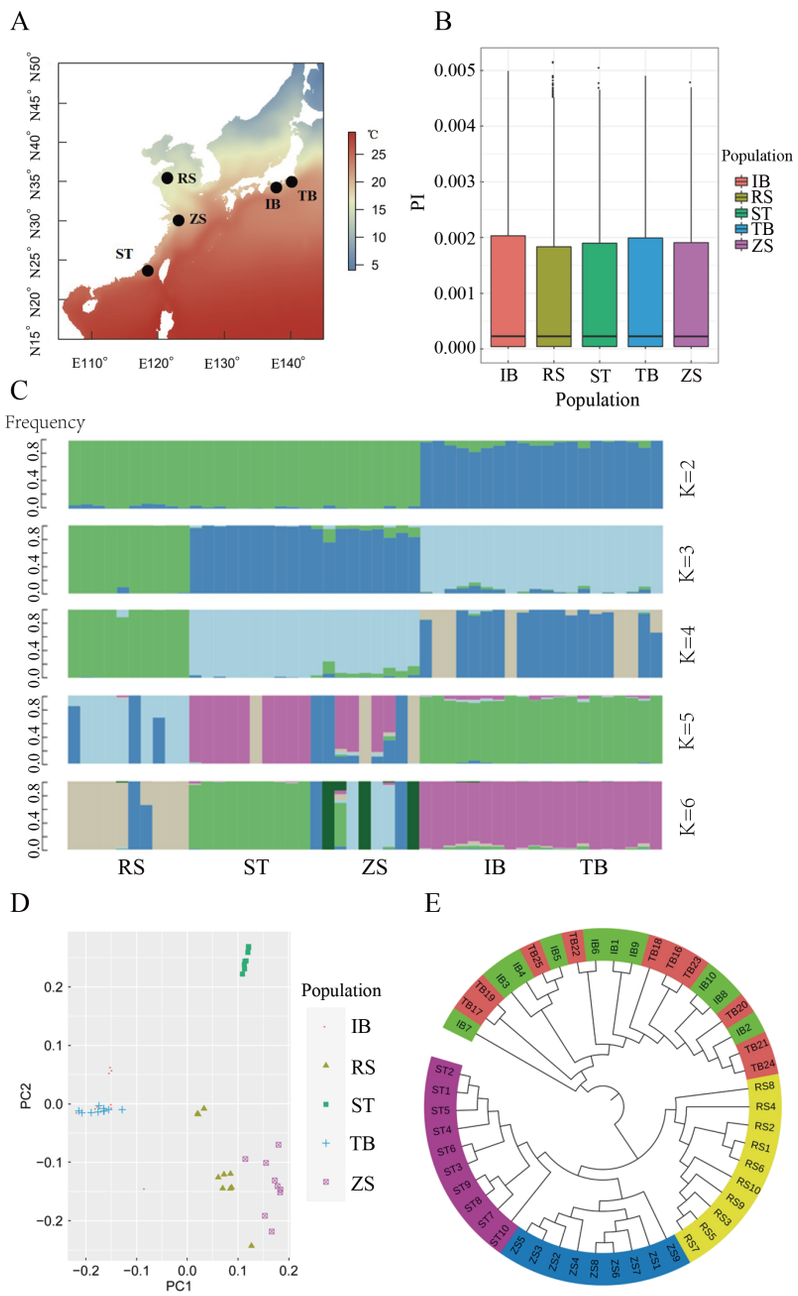

Figure 1 Map of sampling locations and population genomic analyses of *Sillago japonica*

A: Map of sampling locations. Annual sea surface temperature is indicated. B: Genome-wide distribution of nucleotide diversity in 40 kb non-overlapping windows. C: Admixture analysis of five *S. japonica* populations. Length of each colored segment represents proportion of individual genome inferred from ancestral populations (*K*=2–6). D: Principal components 1 (27.80%) and 2 (16.95%) for 49 *S. japonica* individuals. E: Neighbor-joining tree constructed using *p*-distances of 49 *S. japonica* individuals. For abbreviations, see Table 1.

Table 1 Population samples of *Sillago japonica* used in this study

Sample location	Sample ID	Date of collection	Sample size (*n*)	Nucleotide diversity	January temperature (°C)	Mean temperature (°C)	July temperature (°C)	Range (°C)
Rushan	RS	August 2016	10	0.0246±0.0138	7.01	14.9	25.8	18.79
Zhoushan	ZS	June 2016	9	0.0212±0.0120	12.7	19.1	28.1	15.43
Santou	ST	July 2016	10	0.02150±0.0113	24.5	25.2	29.1	4.62
Ise Bay	IB	January 2009	10	0.0208±0.0108	13.5	21.3	27.3	13.75
Tokyo Bay	TB	October 2009	10	0.0213±0.0107	13.0	20.4	27.2	14.14
Total			49					

were aligned to the reference genome (unpublished data) using the Burrows-Wheeler Aligner (BWA) with the option "mem-t 4-k 32 -M" (Li & Durbin, 2009). After mapping, the resulting bam files were sorted using SAMtools (Li et al., 2009) and duplicate reads were removed.

Raw SNPs were identified based on mpileup files generated by SAMtools. The filtering threshold for raw SNPs was set to a quality score of ≥20. The SNPs were discarded if their total coverage was less than one third or greater than five times the overall coverage. If two SNPs were <5 bp apart, both SNPs were removed.

Genomic distribution of genetic variants

ANNOVAR (Wang et al., 2010) was used to annotate the genomic distribution of variants and to classify them into different categories (i.e., nonsynonymous, synonymous, UTR, 5 kb upstream, 5 kb downstream, intronic, and intergenic). The filters for variants were set to a minor allele frequency of >0.01, depth of >3, and missing rate of <0.2.

Population diversity and structure

We used VCFtools (Danecek et al., 2011) to estimate nucleotide diversity (window size of 40 kb) and the F_{ST} divergence statistic (window size of 40 kb) for each population pair. We used Plink (Purcell et al., 2007) (http://pngu.mgh.harvard.edu/~purcell/plink/) to prepare input data for Admixture (Alexander et al., 2009) (http://dalexander.github.io/admixture/index.html) to investigate population structure, with ancestry clusters ranging from two to six. Principal component analysis (PCA) was performed using GCTA software (Yang et al., 2011). The filtered SNP dataset was used to generate neighbor-joining trees with Treebest-1.9.2. Mantel tests, with $F_{ST}/(1-F_{ST})$ and distance matrix analysis performed using the ade4 package (Dray & Dufour, 2007) to test for isolation by distance. Geographical distances among samples were measured by following the coastline (coastal distance) and by the shortest distance across open waters (oceanic distance).

Demographic analysis

The demographic history of all five populations was analyzed using the Pairwise Sequentially Markovian Coalescent (PSMC) model in the PSMC package (Li & Durbin, 2011). In the absence of mutation rates for *S. japonica* or any closely related species, we used a mutation transition matrix based on medaka data (Spivakov et al., 2014). The point mutation rate and recombination rate per base were assumed to be 2.5×10^{-8}. Generation time was calculated as $g=a+(s/(1-s))$, where s is the expected adult survival rate (assumed to be 80%) and a is sexual maturation age (one year for *S. japonica*). A generation time of 5 years was used. To determine the variance in the estimated effective population size, we performed 100 bootstraps for each population. Population-level admixture analysis was conducted using TreeMix v.1.12 (Pickrell & Pritchard, 2012), which inferred the maximum-likelihood (ML) tree for five populations. A window size of 1 000 was used to account for linkage disequilibrium (–k) and "–global" to generate the ML tree. Migration events (–m) were sequentially added to the tree.

Screening for selection signatures

To uncover the genetic variants involved in local adaptation of each population, we calculated the genome-wide distribution of F_{ST} values and π ratios for four control-thermal groups. These groups included the cold-temperature population (RS) vs. control groups (ZS and ST), China warm-temperature population (ZS) vs. control group (RS), and Japan warm-temperature populations (IB and TB) vs. control group (RS). F_{ST} and π for sliding windows were calculated using VCFtools (Danecek et al., 2011), with a window size of 40 kb and a step size of 20 kb. The windows with the top 5% of values for the F_{ST} and π ratios simultaneously served as the candidate outliers under strong selective sweeps. All outlier windows were assigned to their corresponding SNPs and genes. Overlapping genes in cold and warm groups were selected for further analysis to avoid false positives. Selected genes enriched in Gene Ontology (GO) terms and Kyoto Encyclopedia of Genes and Genomes (KEGG) pathways were determined using OmicShare tools (http://www.omicshare.com/tools). Multiple comparisons were corrected using the false discovery rate (FDR-adjusted P-value <0.05). Additionally, PCA was performed to infer the population structure with neutral SNP loci after removing outlier loci.

Distribution prediction of Chinese and Japanese populations under climate change

We used the maximum entropy (Maxent) model (Phillips et al., 2006) to predict potential distributions of two independent populations (Chinese and Japanese) under changing climates. We retrieved species presence records from Zhang et al. (2019) and divided them into Chinese (22 records) and Japanese (23 records) groups. Based on the results of Zhang et al. (2019) and the benthic life type of *S. japonica*, we considered five environmental predictors from Bio-ORACLE (http://www.bio-oracle.org), including ocean depth, distance to shore, mean sea benthic temperature, salinity, and current velocity. The five predictors were not highly correlated (i.e., pairwise Pearson correlation coefficients $|r|<0.70$) and thus all were used to develop the Maxent models. Future (i.e., RCP4.5 in 2100s (average from 2090 to 2100)) marine environmental predictors, including temperature, salinity, and current velocity, were also downloaded from Bio-ORACLE. We assumed that ocean depth and distance to shore would remain unchanged in the future. For each group, we developed a Maxent model using all presence data of the group and present-day environmental predictors; the model was further used to predict potential distributions under present-day and future climatic conditions.

RESULTS

Sequence information and genetic structure

We sampled 49 individuals from five populations covering the East China Sea, Yellow Sea, and Pacific coastal waters of Japan (Figure 1A; Table 1). Whole-genome resequencing yielded 680 Gb of sequencing data and generated 13.6 Gb for each individual. The whole-genome sequence raw reads for *S. japonica* were deposited in the NCBI Sequence Read Archive under accession No. PRJNA743415. Genome alignment

resulted in an average depth of 20.91-fold and average genome coverage of 99.40% (at least one-fold) (Supplementary Table S1). All individual data were aligned to the reference genome (mapping rate from 95.00% to 96.89%) (Supplementary Table S2), and SNPs were called after rigorous quality filtering. We identified 5483086 SNPs after quality control for further analysis, including 406925 in exonic regions, 2025230 in intronic regions, and 2649227 in intergenic regions. Of the exonic SNPs, we identified 312482 synonymous and 94443 nonsynonymous SNPs (Supplementary Table S3). The nucleotide diversity π for each population was similar, ranging from 1.64×10^{-3} to 1.69×10^{-3} (Figure 1B).

Clustering analysis was performed using PLINK and Admixture to examine the relationships among populations (Figure 1C). Admixture analysis revealed clear evidence of clustering. At *K*=2, the admixture structure showed two clusters, with populations from China (RS, ZS, and ST) forming one cluster and populations from Japan (IB and TB) forming another. At *K*=3, the RS population formed a separate cluster. As the *K* value increased, the ST population separated as a unique cluster. When *K* increased from 3 to 6, the ZS population was shared with clusters from RS and ST. Both TB and IB were highly admixed in all cases with *K* from 2 to 6. The PCA results recovered similar clusters as the admixture analyses (Figure 1D). The first principal component (PC1) separated the Chinese and Japanese clades, consistent with the admixture result at *K*=2. The second principal component (PC2) further separated the RS, ZS, and ST populations but was not able to distinguish between the TB and IB populations, consistent with the admixture results at *K*=5 and 6 (Figure 1C). All individuals from the Chinese groups clustered within the population defined by their sampling location, revealing an obvious geographic structure signal from the East China Sea to the Yellow Sea.

The phylogenetic tree further supported the admixture and PCA results. A neighbor-joining tree was constructed based on whole-genome SNPs (Figure 1E). The tree formed two clades that represented geographic divergence between the coastal waters of China and Japan. In the Chinese clade, three distinct clusters generally defined by geographic localities were recovered. However, the phylogenetic topology of the Japanese clade showed a shallow structure, and some individuals were grouped into another geographic population.

We calculated pairwise F_{ST} between populations to quantify their genetic differentiation (Table 2). Pairwise F_{ST} ranged from −0.0001 to 0.0377, with an average of 0.0224, consistent with the overall population structure. Significant F_{ST} values between the Chinese (RS, ZS, and ST) and Japanese populations (IB and TB) ranged from 0.0237 to 0.0377, with an average of 0.0316. The level of genetic differentiation among Chinese populations was higher than that between the two Japanese populations.

Isolation by distance

To explore the influence of geographic distance on genetic differentiation, we performed Mantel tests to determine the association between the geographic distance matrix and pairwise F_{ST} matrix. Two geographic distance patterns (i.e., coastal and oceanic distances) were used in the tests (Figure 2A, B). We identified a closer relationship (r=0.90, *P*=0.0002) between $F_{ST}/(1-F_{ST})$ and coastal distance than that between $F_{ST}/(1-F_{ST})$ and oceanic distance (r=0.80, *P*=0.0029). This indicated isolation due to coastal distance, with coastal distance explaining 91% of the variation in genetic differentiation for the species. Thus, population structure analyses and Mantel tests collectively indicated that strong barriers may have had a greater influence on population differentiation than other factors.

Table 2 Pairwise F_{ST} values for five populations

Sample	RS	ZS	ST	IB
ZS	0.0159*			
ST	0.0214*	0.0177*		
IB	0.0237*	0.0344*	0.0325*	
TB	0.0255*	0.0377*	0.0359*	–0.0001

*: *P*<0.05. For abbreviations, see Table 1.

Demographic history and migration between populations

The demographic history of *S. japonica* was inferred to understand its evolutionary history. Historical effective population sizes were estimated via PSMC. Results showed that the demographic history of *S. japonica* could be traced to ~100 thousand years ago (Ka), and the Chinese and Japanese populations experienced markedly different demographic histories (Figure 2C). The three Chinese populations experienced similar demographic trajectories, with one large population expansion and one population bottleneck. The Chinese populations showed an obvious population expansion ~30 Ka. The effective population size of the Chinese populations peaked ~2–10 Ka, and then declined to a bottleneck ~2 Ka, especially the RS population. Among the three Chinese populations, the population expansion signals increased from north to south, but the bottleneck signal decreased from north to south. The Japanese IB and TB populations showed a different demographic history than the Chinese populations, with only one small population expansion. In contrast to the large and rapid population expansion of the Chinese populations, the Japanese populations started to increase slowly ~10 Ka and reached a peak in present-day.

We reconstructed the ML tree of the five populations using TreeMix to address the population history relationships and identify pairs of populations related to each other independent of that captured by the tree (Figure 2D). The ML tree without migration events inferred from TreeMix analysis divided the 49 individuals into two clusters, similar to the population structuring patterns identified from phylogenetic tree analysis, PCA, and genetic structure analysis. When potential migration edges (i.e., migration events between branches) were added to the ML tree, strong migration events were detected between the clusters (Figure 2E). We observed a significant migration edge (*P*<2.2E–308) with an estimated weight of 28.8%, which provided evidence of gene flow from the Japanese TB population to the RS population.

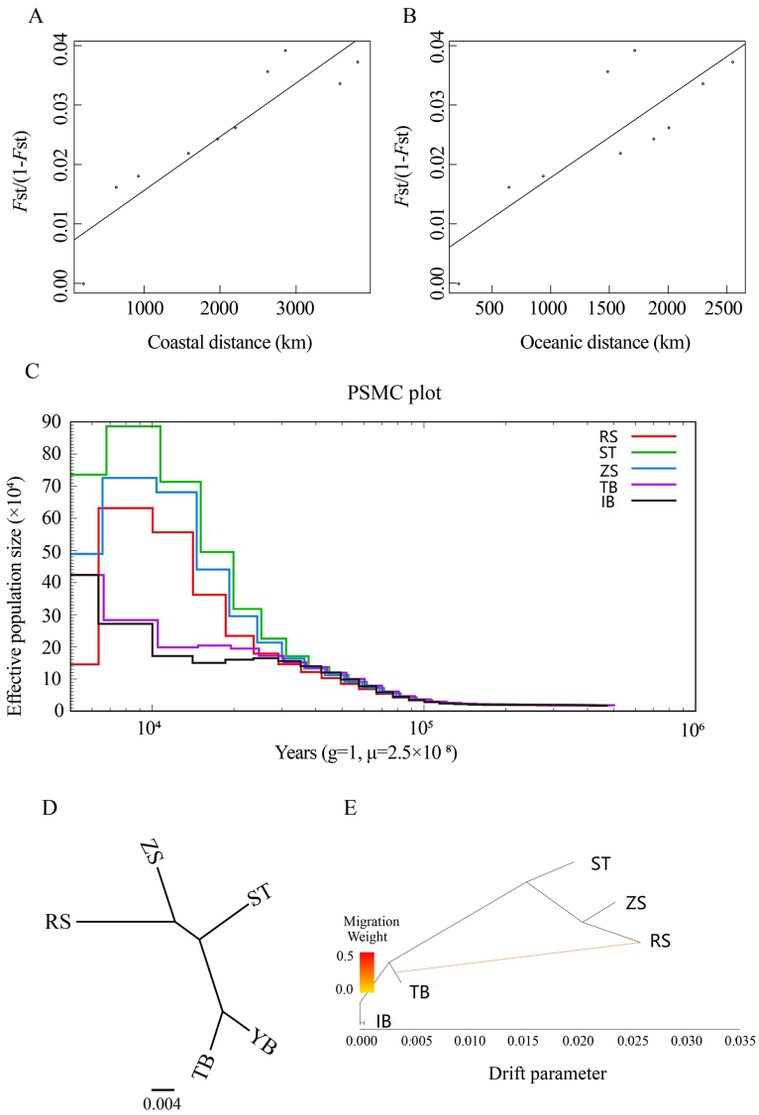

Figure 2 Isolation by distance, demographic history, and pattern of population splits

A, B: Plot of pairwise estimates of $F_{ST}/(1-F_{ST})$ versus two types of geographic distance (i.e., coastal and oceanic distances) between populations. C: Demographic history for each population inferred from PSMC analysis. D, E: Pattern of population splits and mixture between five *S. japonica* populations. Drift parameter is proportional to *Ne* generations, where *Ne* is effective population size. Scale bar shows average standard error of estimated entries in sample covariance matrix.

Genome-wide selection pressure analysis

We compared the genomes of *S. japonica* individuals to identify signatures of positive selection under different environmental selection pressures. Considering that genetic isolation occurred between the Chinese and Japanese populations, we chose the ST and ZS populations as control groups to reveal candidate cold-temperature selection genes in the RS population. Using the top 5% of maximum F_{ST} (F_{ST}≥0.1260) and π ratio ($\Pi_{ST/RS}$≥1.2380) values, a total of 132 candidate genes (corresponding to 3.64 Mb in size) were identified in the RS population when the ST population was used as the control group (Figure 3A). When the ZS population was used as the control group, 509 candidate genes were identified (corresponding to 18.96 Mb) (F_{ST}≥0.0904, $\Pi_{ZS/RS}$≥1.2676). To validate the candidate genes under strong selective sweeps in the RS population, we identified a total of 81 overlapping genes in the RS/ZS and RS/ST pairs as potential genes associated with cold-temperature adaptation for subsequent analyses (Figure 3B; Supplementary Table S4).

To detect possible parallel adaptation between the ZS and IB/TB populations, we identified 692 genes in ZS and 122 genes in the Japanese groups involved in warm-temperature adaptation, with the cold-temperature RS population used as the control group (Figure 3C). Furthermore, 111 of the 122 (91.0%) warm-temperature adaptation genes in the Japanese populations overlapped with the warm-temperature adaptation genes in the ZS population (Supplementary Table S5). Considering the geographic isolation based on whole-genome SNPs and similar temperature environments, the highly

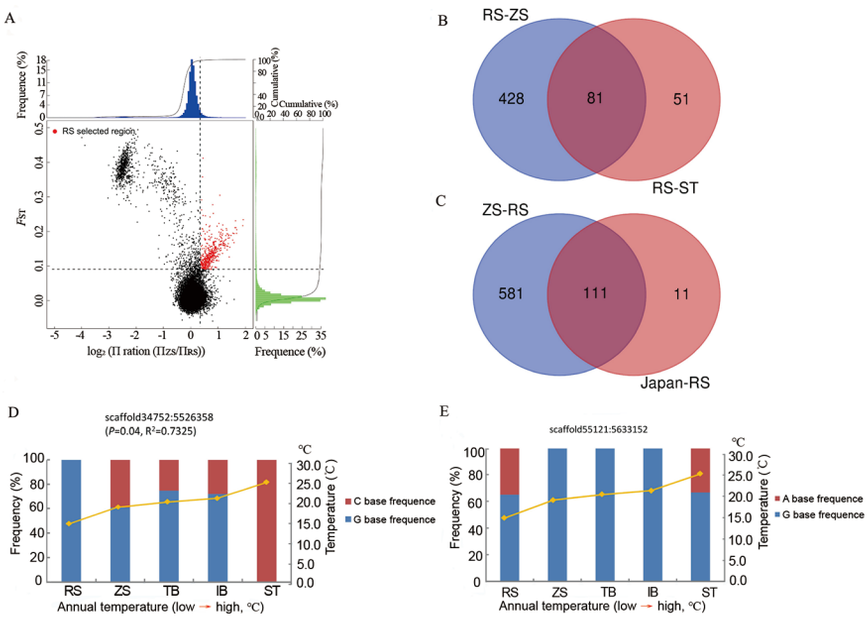

Figure 3 Genomic regions with strong selective signals in populations of *S. japonica*

A: Distribution of $\log_2(\theta_\pi$ ratios) and F_{ST} values calculated in 40 kb sliding windows with 20 kb increments between RS/ZS populations (ZS as control group). Data points in red (corresponding to top 5% of empirical $\log_2[\theta_\pi$ ratio] distributions with values of >0.1204 and top 5% of F_{ST} distributions with values of >0.0904) are genomic regions under selection in RS population. B: Overlapping candidate genes in RS/ZS and RS/ST pairs based on Venn diagram. C: Overlapping candidate genes in ZS/RS and Japan/RS pairs based on Venn diagram. D: Allele frequency of one SNP within cold-temperature adaptation gene *Picalm* across five *S. japonica* populations, red and blue represent two types of bases at this locus. E: Allele frequencies of one SNP within warm-temperature adaptation gene *SORCS3* across five *S. japonica* populations, red and blue represent two types of bases at this locus.

shared selection genes between the Japanese and ZS populations suggest possible parallel adaptive evolution.

The PCA results based on SNPs of candidate genes related to cold-temperature adaptation indicated that individuals from the RS population were separated from other populations (Figure 4A). PC1 tended to separate populations with different latitudes from south to north, while PC2 separated RS from the other populations. The allele frequency of one SNP within the cold-temperature adaptation gene *Picalm* was significantly associated with population temperature (Figure 3D). However, the allele frequencies of one SNP within the warm-temperature adaptation gene *SORCS3* showed high values in the three warm-temperature populations (Figure 3E).

The PCA results based on SNPs of candidate genes related to warm-temperature adaptation also divided the 49 individuals into two clades between the ST population and the other four populations, with the RS population at the intermediate position (Figure 4B). This topological pattern was different from that inferred from the genome-wide SNPs (Figure 1D), thus supporting the credibility of the candidate genes under selection. The PCA substructure based on the candidate parallel genes related to warm-temperature adaptation revealed a closer relationship between the ZS populations and IB/TB pair than with genome-wide SNPs (Figure 4B). We filtered the SNP data after removing outlier loci from both cold and warm adaptive regions. The PCA results based on neutral SNP loci were similar to that obtained from the total loci (Supplementary Figure S1).

To obtain a broad overview of the molecular functions of these genes and detect the most differentiated regions of the *S. japonica* genome, we performed GO and KEGG enrichment analyses on the candidate selection genes. These analyses offered clear insight into the genetic evolution and adaptive mechanisms of *S. japonica* under different thermal environments.

Functional enrichment indicated that the candidate genes under cold selection were significantly enriched in only one KEGG pathway, i.e., choline metabolism in cancer (ko05231, FDR-adjusted P=0.042 1) (Figure 4C; Supplementary Table S6). However, GO term enrichment analysis of the 81 candidate genes under cold-temperature selection classified the genes into 47 categories, including metabolic processes, biological regulation, response to stimulus, and signaling process in the biological process, membrane and membrane part in the cellular component, and binding and catalytic activity in the molecular function (Supplementary Figure S2). We found 50 significantly enriched GO terms after FDR correction (Supplementary Figure S3 and Table S7). The significantly enriched GO categories were primarily associated with cell part, cation transmembrane transporter activity, tissue homeostasis, transport, and lipid metabolism.

In total, 111 genes were identified for parallel adaptations in the ZS, IB, and TB populations. These genes were classified into 48 categories (Supplementary Figure S4), including 19 significantly overrepresented GO categories detected for thermal adaptation (Supplementary Table S8). The GO clusters were primarily enriched in cell projection, structure of the cytoskeleton, binding, and maintenance of the membrane

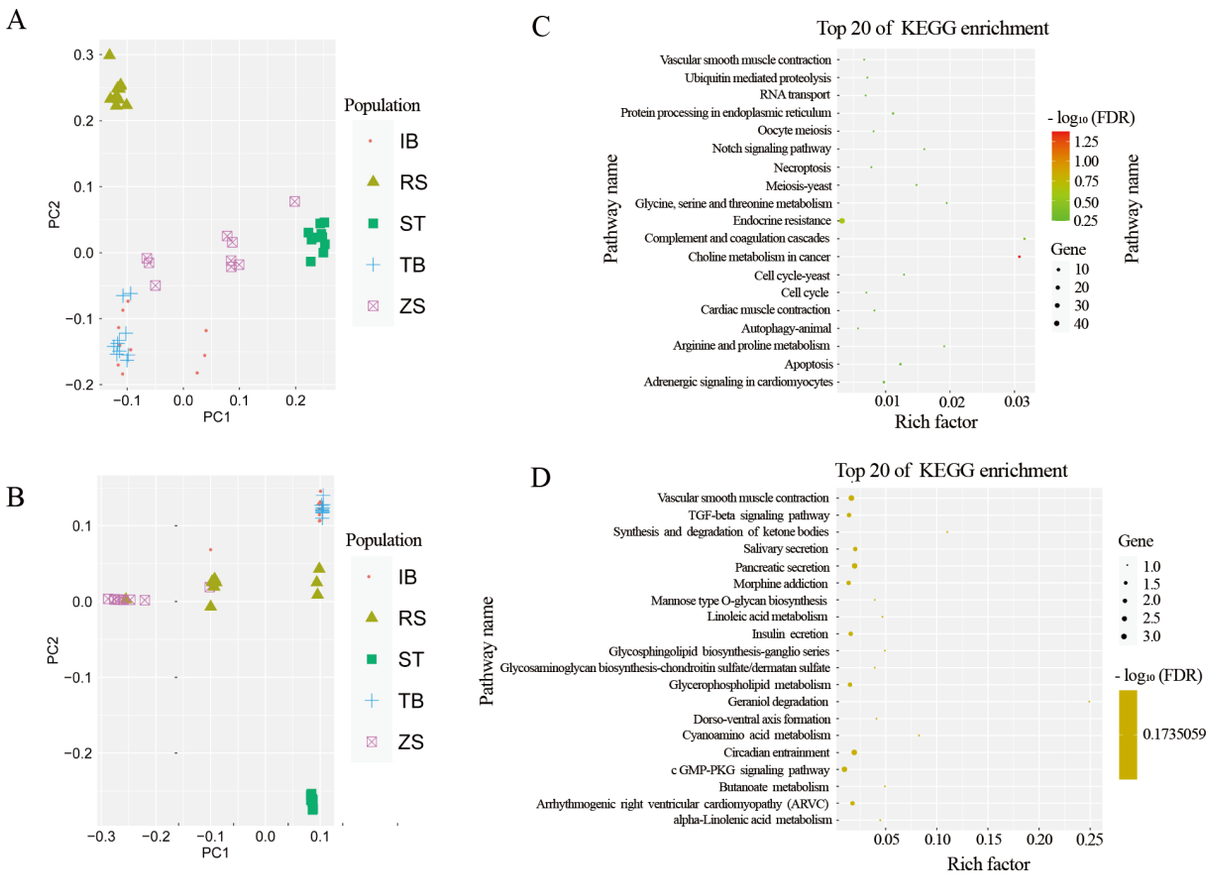

Figure 4 PCA based on SNPs located in candidate genes and top 20 enriched KEGG pathways in candidate genes

A: PCA based on cold-temperature adaptation genes. B: PCA based on warm-temperature adaptation genes. C: KEGG enrichment for cold-temperature adaptation genes. D: KEGG enrichment for warm-temperature adaptation genes.

(Supplementary Figure S2). Although no significantly enriched KEGG pathways were detected, the top 20 enriched pathways were related to metabolism (synthesis and degradation of ketone bodies, cyanoamino acid metabolism, linoleic acid metabolism, alpha-linolenic acid metabolism, and butanoate metabolism), circulatory system (vascular smooth muscle contraction), and endocrine system (salivary secretion and pancreatic secretion) (Figure 4D; Supplementary Table S9). Enrichment of the selected genes in the warm-temperature population suggested a parallel adaptive mechanism to cold temperature.

Distribution prediction of Chinese and Japanese populations by Maxent model

Based on receiver operating characteristic (ROC) analysis, the area under the ROC curve (AUC) results (0.983 in Chinese group, 0.995 in Japanese group) suggested that the Maxent model showed good predictive performance. The Maxent predictions for the two *S. japonica* groups suggested that the potential distribution of this species may change substantially (Figure 5). The predictions showed that large areas of coastal China, central Japan, and Korea were suitable for the Chinese group (Figure 5A). However, more suitable distribution areas for the Japanese group were only in southern and central Japan (Figure 5E). The northern boundary for the potential population distribution of the Japanese group in the East China Sea was Zhoushan. Climate change is predicted to influence the two groups differently. Under a future RCP4.5 scenario, habitat suitability for the Chinese group would clearly increase from south to north and potential distribution may shift northward along the coastal waters of China and Japan by 2100 (Figure 5B, G). However, results also revealed a reduction in the potential area for the Japanese group and no clear increase in areas of northern Japan by 2100 (Figure 5F, G). This predicted reduction in habitat suitability may indicate lower evolutionary potential to adapt to changing environments. The response curves to temperature suggested different temperature adaptations between the two groups, with the Chinese group preferring high temperatures and the Japanese group favoring low temperatures (Figures 5D, H).

DISCUSSION

New insight on genetic structure of *S. japonica*

Both historical and current variable environments have had profound effects on the genetic variation of species. Analyses at the genomic level can provide detailed information on the genetic structure, population history, and adaptation of species to various environments, which can facilitate their protection and management (Li et al., 2019). Here, based on population genomics, we delineated the genetic

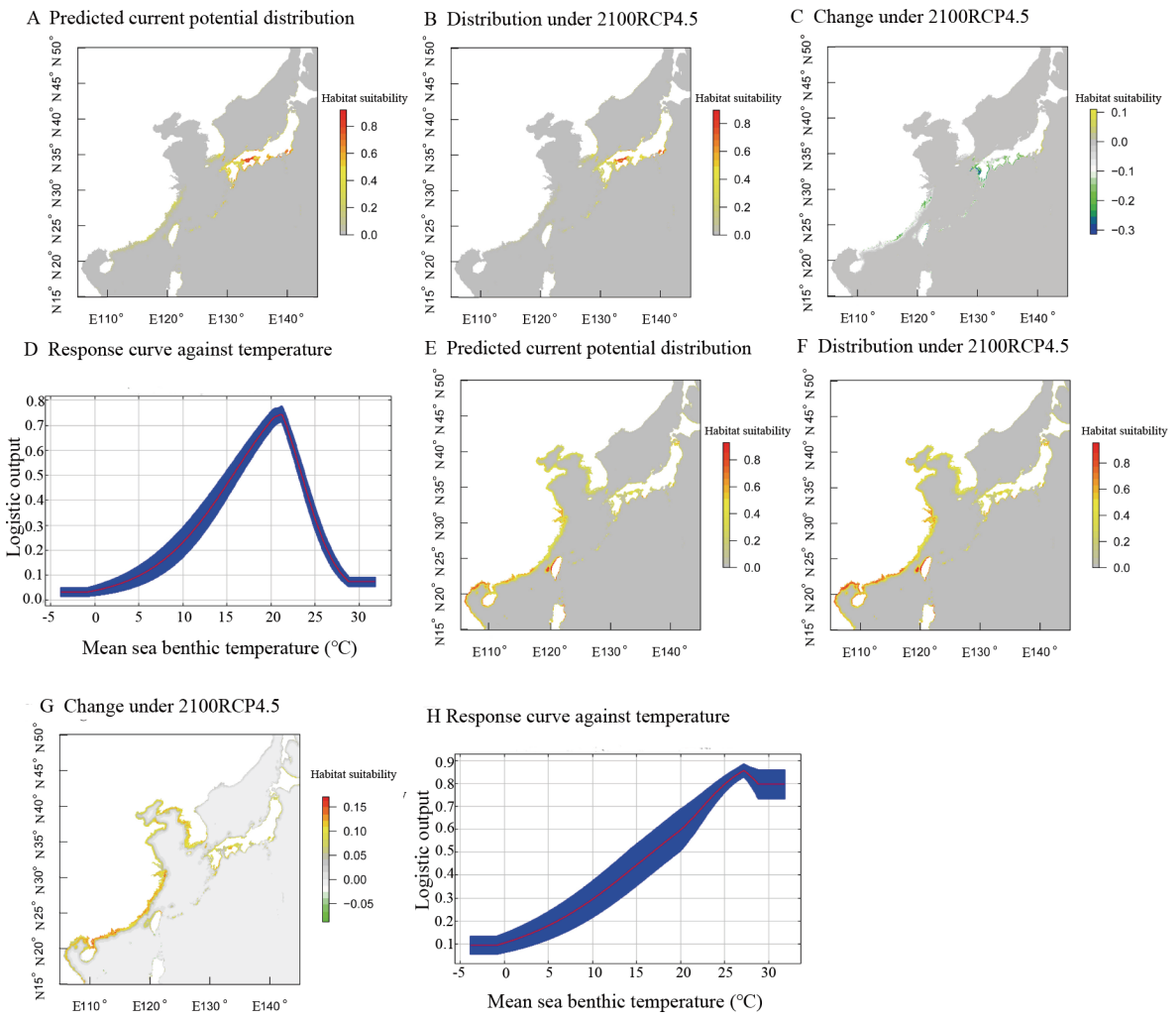

Figure 5 Predicted potential distribution (A, B), changes in habitat suitability (C) of Chinese group under RCP45 scenarios, and response curves of predicted occurrence probability (D) of Chinese group against temperature. Predicted potential distribution (E, F), changes in habitat suitability (G) of Japanese group under RCP45 scenarios, and response curves of predicted occurrence probability (H) of Japanese group against temperature

characteristics of *S. japonica* populations via whole-genome sequencing. To the best of our knowledge, this is the first study to adopt whole-genome sequencing to assess population differentiation and selection signatures in a marine fish species in the northwestern Pacific. Population history analyses suggested that the historical sea level had a substantial influence on the effective population size of this species, with a warmer climate facilitating population growth. We also identified several genes related to local environment adaptation.

Our study also provided a higher population structure resolution than that found in previous studies based on GBS, mtDNA control region, and morphological data (Gao et al., 2019; Xue et al., 2010). For example, using morphological analysis of *S. japonica*, Xue et al. (2010) found no significant differentiation among populations from the Yellow Sea, East China Sea, and South China Sea. In addition, using the mtDNA control region to explore genetic differentiation, Gao et al. (2019) detected no genetic structure in *S. japonica* due to the short fragment of this region. Using GBS technology, Yang et al. (2020) observed considerable genetic differentiation between the Chinese and Japanese populations of *S. japonica* but failed to separate individuals from these populations. In contrast to the mtDNA and GBS results, our study revealed a complete genetic break between the Chinese and Japanese populations according to whole-genome sequencing data. Furthermore, PCA distinguished the three Chinese populations.

Pleistocene glaciations are considered important events that shaped the phylogeographic genetic structures of extant species (Han et al., 2018). The divergence between the Chinese and Japanese populations may reflect historical isolation between the East China Sea and Pacific Ocean during the Pleistocene low sea-level stands. In the present study, population demographic analysis suggested a divergence time of 30 Ka between the two clades during the last glacial period. The date of divergence was consistent with geological events that may have created a vicariant barrier between the *S. japonica* populations of the Pacific Ocean and East China Sea (Kawahata & Ohshima, 2004).

Mantel tests identified a strong relationship between coastline distance and genetic differentiation. The ocean distance that separates the western and eastern East China Sea was identified as a physical barrier that restricted gene flow between samples. Considering the life history of this species and the physical environment in the East China Sea, long ocean distance is a reasonable physical barrier for a demersal species. Furthermore, ocean depth (<30 m) is known to limit the distribution of *S. japonica* in marine waters (https://www.fishbase.in/summary/Sillago-japonica.html). The average depth of the East China Sea is about 370 m, with a maximum of 2 719 m at the continental slope (Guan & Mao, 1982). Therefore, the depth of water along the direct dispersal route between the coastal waters of China and Japan may have formed an unsuitable habitat for this species and prevented its offshore dispersal. Historical migration events from the TB to RS populations and lack of migration from the Japanese populations to the ZS population support a coastal dispersal pattern. This pattern is also supported by the potential distribution areas of the two groups predicted by the Maxent model. A coastal dispersal pattern has also been observed in Japanese grenadier anchovy (*Coilia nasus*) (Gao et al., 2014; Han et al., 2015), a species with similar biological characteristics and geographical distribution in the East China Sea as *S. japonica*. Notably, amplified fragment length polymorphism (AFLP) and mtDNA analysis of *C. nasus* suggested that direct ocean distance with deep water at the continental slope between the western and eastern coastal waters of the East China Sea served as a major physical barrier to this species.

The different demographic histories between the Chinese and Japanese populations may have resulted from geographic and climatic differences. The three Chinese populations showed an obvious and rapid population expansion ~30 Ka. In contrast, the Japanese populations started to increase slowly ~10 Ka, reaching a peak at present-day. Moreover, the TB and IB populations showed a slower rate of increase compared with the Chinese populations over the same time. The coastal waters of Japan, with no serious historical sea-level rises, experienced less impact during the Pleistocene glaciations. The expansions of the Chinese and Japanese populations are consistent with historical sea-level increases during the interglacial periods. Notably, the populations started to increase dramatically ~30 Ka when the Wurm glacial stage began to end in the northwestern Pacific (Kawahata & Ohshima, 2004).

Pelagic and demersal fish in the coastal waters of China are expected to exhibit little intraspecific genetic structuring due to the ocean currents and apparent lack of physical barriers (Han et al., 2008). Given its wide distribution and ecological characteristics, *S. japonica* may be susceptible to heterogeneous local environments. Likewise, genome-wide SNP studies have revealed remarkable regional differentiation between northern and southern populations of rough-skin sculpin (*Trachidermus fasciatus*), marbled rockfish (*Sebastiscus marmoratus*), spotted seabass (*Lateolabrax maculatus*), and small yellow croaker (*Larimichthys polyactis*) (Li et al., 2019; Liu et al., 2016; Xu et al., 2017). Thus, due to local adaptations to heterogeneous environments, a high degree of regional differentiation between northern and southern Chinese populations may be common in marine fish. For instance, average annual sea surface temperatures range from 15.9 °C in the RS population to 25.2 °C in the ST population (data provided by the Bio-ORACLE). This obvious difference in the thermal environment may have resulted in divergent selection on specific genes, and genetic diversity in certain genomic regions would be substantially decreased due to natural selection.

Adaptive mechanisms for cold temperature

Understanding how ecological variants of fish can affect population structure will have comprehensive implications for conservation management and decision-making (Li et al., 2019). Water temperature is one of the most important abiotic factors that influence the phenotypes and habitats of aquatic organisms (Chen et al., 2018b). As an important environmental stressor, low temperatures can have broad biological effects on marine organisms. These thermal effects can generate intense selective pressure on genes and genomic regions.

In the current study, selective sweep analysis was conducted to identify thermally affected genes between the northern and southern populations of *S. japonica*. Combining alternative statistical approaches to detect selection signatures can provide more robust results by decreasing false-positive rates. We evaluated the genetic attributes of candidate genes relative to the genomic background. We scanned the genome-wide variations using F_{ST} values and π ratios.

A total of 81 candidate genes in the RS population identified by both π ratio and F_{ST} analyses were recognized as potentially affected genes related to cold adaptation. Cold adaptation and acclimatization studies suggest that more than one mechanism is involved in the biological response to cold stress (Liu et al., 2018; White et al., 2012). As expected, based on the biological complexity of cold adaptation, several different processes, rather than one term or pathway, were identified by our selection tests. Low temperatures can influence energy metabolism. Here, four selection genes (low-density lipoprotein receptor (*LDLR*), *ZBTB20*, *PICALM*, and *nup35*) were related to the lipid metabolic process. Lipids are the main components of the cytomembrane (van Meer et al., 2008). A common cold adaptation mechanism for the cell is to manipulate the membrane lipid composition to maintain membrane fluidity and, correspondingly, proper membrane permeability and function of protein complexes (e.g., transporters) (Russell & Nichols, 1999).

Previous studies have shown that cell membrane permeability, integrity, and stability can be damaged under long-term low-temperature conditions (Cardona et al., 2014; Liu et al., 2018). *LDLR* is an important candidate gene for cold adaptation. As a glycoprotein located on the surface of cells, *LDLR* mediates the endocytic uptake of low-density lipoprotein (LDL) cholesterol in the liver and is a key metabolic regulator of plasma LDL cholesterol (Yamamoto et al., 1984). *LDLR* is the most powerful determinant of variation in total and LDL cholesterol levels (Hansen et al., 1997). This gene also plays an essential role in protecting cell membrane integrity under

cold stress and strong selection pressure on this gene is useful for low-temperature adaptation (Dong et al., 2013). Similar results have also been observed for the low-density lipoprotein receptor-related protein 5 (*LRP5*) gene (Cardona et al., 2014). *LRP5* shows strong signals of selection in indigenous Siberian human populations, exhibits high expression in the liver, and plays a role in cholesterol metabolism. Natural selection of the *LRP5* gene helps Siberians to cope with cold climates (Cardona et al., 2014). An elevated basal metabolic rate is also a cold adaptation strategy. The selection gene *TPO* is involved in thyroid metabolism (Leonard et al., 2005), which determines the basal metabolic rate of the body. Thus, natural selection of the *TPO* gene in the RS population may maintain the basal metabolic rate under cold stress.

We also detected substantial adaptive evidence concerning ion exchange and transportation, which are processes that affect the fluidity and permeability of the cell membrane and are directly and indirectly linked to thermal regulation (Maksimov et al., 2017). We identified numerous genes that encode transporters (e.g., MFS transporters *SLC22A5*, *SLC7A2*, and *SLC25A5*) and ion channels (e.g., voltage-gated sodium channel *SCN4B*) in genomic regions of the RS population under selective sweeps. For example, we identified four copies of *SLC22A5* in the genome of *S. japonica*, thus indicating gene expansion. *SLC22A5* is a specific transporter found in cell membranes and mitochondria and is involved in the uptake and release of carnitine (Wu et al., 1999). Carnitine is a carrier of long-fatty acids and facilitates their transport into the mitochondria for lipid oxidation. Defective *SLC22A5* causes systemic carnitine deficiency, resulting in metabolic decompensation (Hu et al., 2018). Furthermore, the *SLC7A2* gene functions as a permease involved in transporting cationic amino acids across the plasma membrane (Closs et al., 1997). These transporter and ion channel genes are crucial for transmembrane transport to maintain stability between the internal and external environments of cells under cold temperature. Therefore, genes that encode transcellular ion transporters and channel proteins can be reshaped by natural selection under cold stress environments.

Smooth muscle contraction, which includes vasoconstriction and vasodilation, is also implicated in cold adaptation (Cardona et al., 2014). We identified two genes involved in this process that showed evidence of strong selection signals, i.e., *CPI17* (protein phosphatase 1 regulatory subunit 14A) and *CACNB4*. *CPI17* is an inhibitor of PPP1CA and shows >1 000 -fold inhibitory activity when phosphorylated, creating a molecular switch for regulating the phosphorylation of PPP1CA substrates and smooth muscle contraction in the absence of increased intracellular Ca^{2+} (Li et al., 2001). The *CACNB4* gene encodes a calcium channel subunit expressed in the heart and increases the peak calcium current, which is important for cardiac muscle contraction under cold stress (Rouhiainen et al., 2016). Although no heart rate data are available for the studied populations, cold exposure is known to increase cardiac pressure. Thus, efficient cardiovascular regulation may be a possible cold adaptive mechanism in the RS population. These genetic changes may facilitate the adaptation and survival of *S. japonica* in low-temperature areas.

Cell repair and clear necrotic organelles are also important processes of cold adaptation, as found in the RS population. We identified two important genes under natural selection involved in cell repair. Interferon regulatory factor 1 (*IRF1*) is a transcriptional regulator that displays remarkable functional diversity in regulating cellular responses (Oshima et al., 2004). Under cold stress, *IRF1* causes cells to suspend proliferation to survive adverse environmental conditions and triggers apoptosis when cell damage becomes irreparable, thereby preventing harmful cells from damaging normal cells. DnaJ homolog subfamily C member 10 is involved in the correct folding of proteins and the degradation of misfolded proteins (Oka et al., 2013). It also promotes the apoptotic signaling pathway in response to endoplasmic reticulum stress.

Functional enrichment analysis identified 50 significant GO terms and one KEGG pathway after FDR adjustment. The enriched categories and pathways were primarily associated with cell part, transmembrane transporter activity, tissue homeostasis, lipid metabolism, apoptosis, and vascular smooth muscle contraction. These functional clusters are biologically relevant to cold adaptations and essential in regulating mechanisms for fish to respond to cold environments.

Evidence of parallel evolution in several warm-temperature adaptation genes

In general, geographically distinct populations exposed to similar environmental conditions evolve similar genotypic and phenotypic traits. The replicated nature of *S. japonica* provides clear molecular signatures that can be used to recover alleles consistently associated with parallel warm-temperature adaptations between the ZS and IB/TB populations, despite different historical population origins. In the present study, most local adaptation genes (91.0%) in the Japanese populations were shared with selection genes in the ZS population, with the populations spanning long geographic distances but showing similar annual temperatures (19.1–21.3 ℃). The integration of shared selection genes and similar temperature environments could be considered as possible evidence for parallel evolution in *S. japonica*. The PCA results based on the SNPs of the shared selection genes revealed close but distinguishable patterns between the ZS and two Japanese populations, indicating independent selection events on the same genes between the ZS and IB/TB populations. Similarly, fixation of different loci at the same gene has been reported in marine-freshwater divergence of the three-spine stickleback (Barrett et al., 2008). Evidence of parallel evolution at *TSHR*, a major gene associated with reproductive timing, has also been observed between Atlantic herring populations from both sides of the Atlantic Ocean (Lamichhaney et al., 2017). Parallel genetic evolution has also been reported in the Atlantic cod and *Sebastiscus marmoratus* (Bradbury et al., 2010; Xu et al., 2019).

Here, *S. japonica* was studied to explore the genetic basis of repeated parallel evolution and to identify local adaptation genes in geographically distant and independent populations. Candidate genes were identified within peaks of parallel divergence between the ZS and IB/TB populations. These candidate genes may be important for local adaptation.

Furthermore, GO clusters were primarily enriched in categories related to cell projection, structure of the cytoskeleton, protein binding, maintenance of membrane, and cell differentiation. In addition, although no KEGG pathway showed significant enrichment, the top 20 enriched KEGG pathways were related to metabolism (synthesis and degradation of ketone bodies, cyanoamino acid metabolism, linoleic acid metabolism, alpha-linolenic acid metabolism, and butanoate metabolism), circulatory system (vascular smooth muscle contraction), and endocrine system (salivary secretion and pancreatic secretion).

As subtropical/tropical origin *S. japonica* is adapted to higher temperatures, warm temperature exerts relaxed selection pressure on genes involved in heat stress responses. Moreover, warm temperatures would likely promote *S. japonica* growth by increasing cell membrane fluidity, rapid cell division, and extracellular/intracellular substance exchange. In the current study, among the candidate genes for warm-temperature adaptation, four genes were related to cell division (GO: 0051301), 17 genes were related to cytoskeleton (GO: 0016328), 10 genes were related to transmembrane signaling receptor activity (GO: 0004888), and eight genes were related to ion transmembrane transport (GO: 0034220). Various receptors in the membrane and ion transmembrane transport genes play important roles in the material exchange between the internal and external environments of cells to satisfy rapid cell division. We also identified three genes (*FMN2*, *MGMT*, and *POLH*) that were related to DNA repair (GO: 0006281), thus helping to avoid DNA replication errors. *FMN2* plays a role in responding to DNA damage, cellular stress, and hypoxia by protecting CDKN1A against degradation. *FMN2* also promotes the assembly of nuclear actin filaments in response to DNA damage to facilitate the movement of chromatin and repair factors after DNA damage (Yamada et al., 2013). *MGMT* is crucial for genome stability. It repairs the naturally occurring mutagenic DNA lesion O6-methylguanine back to guanine and prevents mismatch and errors during DNA replication and transcription (Kawate et al., 2000). *POLH* serves as a DNA polymerase specifically involved in DNA repair by translesion synthesis (Masutani et al., 1999). Warm temperature promotes material exchange, DNA replication, and cell division. Furthermore, suitable temperature ensures that enough food resources are available in the environment. Hence, the above terms are functionally necessary for the adaptations of *S. japonica* to warm temperatures.

Different climate resilience between Chinese and Japanese groups

Natural selection analysis demonstrated that the different populations exhibited different temperature adaptability at the genetic level. We also obtained evidence of differences in temperature adaptation between the Chinese and Japanese populations at the macro level through species distribution models. The differences in the potential distributions of the two groups under future climate change may reflect the different thermal abilities between the groups. The Chinese group contained different thermally adapted populations, which may possess strong adaptive capacities to future climate change. However, the Japanese group with stenothermal characteristics showed weak adaptive capacity to climate change. Our findings are different from the predicted distribution of this species reported by Zhang et al. (2019), who did not consider genetic differences within this species. Cryptic diversity clearly affects global climate change projections. Bálint et al. (2011) suggested that without discerning intraspecific genetic variation and cryptic diversity, the effects of global climate change are likely to be drastically underestimated. From our findings, the phylogeographic data and species distribution models provide a new understanding of the evolutionary trajectories of species under changing environmental conditions.

CONCLUSIONS

Based on the neutral and total SNPs, we identified two isolated populations that showed strong parallel evolution. This genetic parallelism was likely due to the similar local temperature environments, notwithstanding the different thermal origins of the populations. The population-specific genes related to adaptations to low temperatures may be considered as potential candidates for further exploration of the underlying mechanisms involved in confronting environmental challenges. In conclusion, by comparing the whole genomes of *S. japonica* populations from different temperature regions, we revealed various genes associated with local adaptations to cold temperature environments. Specifically, candidate genes were functionally related to membrane fluidity in cold environments. These results advance our understanding of the underlying genetic mechanisms that allow fish, especially small ruminants, to adapt to extreme environments.

SUPPLEMENTARY DATA

Supplementary data to this article can be found online.

COMPETING INTERESTS

The authors declare that they have no competing interests.

AUTHORS' CONTRIBUTIONS

S.J.X. and T.X.G. conceived and supervised the study. T.X.G. performed sample collection. X.Y.G. conducted DNA extraction and genome sequencing. Q.L. conducted SNP calling and genetic diversity analysis. S.S.L. performed PCA. Z.Q.H. analyzed the population genetic structure, demographic history, and selection signatures, and wrote the draft manuscript. Z.X.Z performed species distribution model analysis. All authors read and approved the final version of the manuscript.

ACKNOWLEDGMENTS

We thank Sheng-You Xu (Zhejiang Ocean University) and Fang-Rui Lou (Ocean University of China) for valuable suggestions and comments.

REFERENCES

Alexander DH, Novembre J, Lange K. 2009. Fast model-based estimation of ancestry in unrelated individuals. *Genome Research*, **19**(9): 1655−1664.

Assis J, Tyberghein L, Bosch S, Verbruggen H, Serrão EA, De Clerck O.

2018. Bio-ORACLE v2.0: Extending marine data layers for bioclimatic modelling. *Global Ecology and Biogeography*, **27**(3): 277−284.

Balanyà J, Huey RB, Gilchrist GW, Serra L. 2009. The chromosomal polymorphism of *Drosophila subobscura*: a microevolutionary weapon to monitor global change. *Heredity*, **103**(5): 364−367.

Bálint M, Domisch S, Engelhardt CHM, Haase P, Lehrian S, Sauer J, et al. 2011. Cryptic biodiversity loss linked to global climate change. *Nature Climate Change*, **1**(6): 313−318.

Barrett RDH, Rogers SM, Schluter D. 2008. Natural selection on a major armor gene in threespine stickleback. *Science*, **322**(5899): 255−257.

Bradbury IR, Hubert S, Higgins B, Borza T, Bowman S, Paterson IG, et al. 2010. Parallel adaptive evolution of Atlantic cod on both sides of the Atlantic Ocean in response to temperature. *Proceedings of the Royal Society B: Biological Sciences*, **277**(1701): 3725−3734.

Cai RS, Han ZQ, Yang ZX. 2020. Impacts and risks of changing ocean on marine ecosystems and dependent communities and related responses. *Climate Change Research*, **16**(2): 182−193. (in Chinese)

Cardona A, Pagani L, Antao T, Lawson DJ, Eichstaedt CA, Yngvadottir B, et al. 2014. Genome-wide analysis of cold adaptation in indigenous Siberian populations. *PLoS One*, **9**(5): e98076.

Chen C, Wang HH, Liu ZG, Chen X, Tang J, Meng FM, et al. 2018a. Population genomics provide insights into the evolution and adaptation of the eastern honey bee (*Apis cerana*). *Molecular Biology and Evolution*, **35**(9): 2260−2271.

Chen ZQ, Farrell AP, Matala A, Hoffman N, Narum SR. 2018b. Physiological and genomic signatures of evolutionary thermal adaptation in redband trout from extreme climates. *Evolutionary Applications*, **11**(9): 1686−1699.

Closs EI, Gräf P, Habermeier A, Cunningham JM, Förstermann U. 1997. Human cationic amino acid transporters hCAT-1, hCAT-2A, and hCAT-2B: three related carriers with distinct transport properties. *Biochemistry*, **36**(21): 6462−6468.

Danecek P, Auton A, Abecasis G, Albers CA, Banks E, DePristo MA, et al. 2011. The variant call format and VCFtools. *Bioinformatics*, **27**(15): 2156−2158.

Dong M, Yang XY, Lim S, Cao ZQ, Honek J, Lu HX, et al. 2013. Cold exposure promotes atherosclerotic plaque growth and instability via UCP1-dependent lipolysis. *Cell Metabolism*, **18**(1): 118−129.

Dray S, Dufour AB. 2007. The ade4 package: Implementing the duality diagram for ecologists. *Journal of Statistical Software*, **22**(4): 1−20.

Ferchaud AL, Hansen MM. 2016. The impact of selection, gene flow and demographic history on heterogeneous genomic divergence: three-spine sticklebacks in divergent environments. *Molecular Ecology*, **25**(1): 238−259.

Fustier MA, Brandenburg JT, Boitard S, Lapeyronnie J, Eguiarte LE, Vigouroux Y, et al. 2017. Signatures of local adaptation in lowland and highland teosintes from whole-genome sequencing of pooled samples. *Molecular Ecology*, **26**(10): 2738−2756.

Gao TX, Wan ZZ, Song N, Zhang XM, Han ZQ. 2014. Evolutionary mechanisms shaping the genetic population structure of coastal fish: insight from populations of *Coilia nasus* in Northwestern Pacific. *Mitochondrial DNA*, **25**(6): 464−472.

Gao TX, Yang TY, Yanagimoto T, Xiao YS. 2019. Levels and patterns of genetic variation in Japanese whiting (*Sillago japonica*) based on mitochondrial DNA control region. *Mitochondrial DNA Part A*, **30**(1): 172−183.

Guan BX, Mao HL. 1982. A note on circulation of the East China Sea. *Chinese Journal of Oceanology and Limnology*, **1**(1): 5−16.

Han ZQ, Gao TX, Yanagimoto T, Sakurai Y. 2008. Deep phylogeographic break among white croaker *Pennahia argentata* (Sciaenidae, Perciformes) populations in North-western Pacific. *Fisheries Science*, **74**(4): 770−780.

Han ZQ, Han G, Wang ZY, Gao TX. 2015. The possible physical barrier and coastal dispersal strategy for Japanese grenadier anchovy, *Coilia nasus* in the East China Sea and Yellow Sea: Evidence from AFLP Markers. *International Journal of Molecular Sciences*, **16**(2): 3283−3297.

Han ZQ, Wang ZY, Gao TX, Yanagimoto T, Iida K. 2018. Assessing the speciation of a cold water species, Japanese sand lance *Ammodytes personatus*, in the Northwestern Pacific by AFLP Markers. *Animals*, **8**(12): 224.

Hansen PS, Defesche JC, Kastelein JJP, Gerdes LU, Fraza L, Gerdes C, et al. 1997. Phenotypic variation in patients heterozygous for familial defective apolipoprotein B (FDB) in three European countries. *Arteriosclerosis, Thrombosis, and Vascular Biology*, **17**(4): 741−747.

Hu CW, Hu CH, Wu-Chou YH, Lo LJ. 2018. SLC22A5 mutations in a patient with systemicprimary carnitine deficiency and cleft palate-successful perioperative management. *Journal of Craniofacial Surgery*, **29**(6): 1601−1603.

Kashiwagi K, Kondo S, Yoshida W, Yoshioka M. 2000. Effects of temperature and salinity on hatching success of Japanese whiting *Sillago japonica* eggs. *Aquaculture Science*, **48**(4): 637−642.

Kawahata H, Ohshima H. 2004. Vegetation and environmental record in the northern East China Sea during the late Pleistocene. *Global and Planetary Change*, **41**(3–4): 251−273.

Kawate H, Itoh R, Sakumi K, Nakabeppu Y, Tsuzuki T, Ide F, et al. 2000. A defect in a single allele of the *Mlh1* gene causes dissociation of the killing and tumorigenic actions of an alkylating carcinogen in methyltransferase-deficient mice. *Carcinogenesis*, **21**(2): 301−305.

Lamichhaney S, Fuentes-Pardo AP, Rafati N, Ryman N, McCracken GR, Bourne C, et al. 2017. Parallel adaptive evolution of geographically distant herring populations on both sides of the North Atlantic Ocean. *Proceedings of the National Academy of Sciences of the United States of America*, **114**(17): E3452−E3461.

Leonard WR, Snodgrass JJ, Sorensen MV. 2005. Metabolic adaptation in indigenous Siberian populations. *Annual Review of Anthropology*, **34**: 451−471.

Li H, Durbin R. 2009. Fast and accurate short read alignment with Burrows-Wheeler transform. *Bioinformatics*, **25**(14): 1754−1760.

Li H, Durbin R. 2011. Inference of human population history from individual whole-genome sequences. *Nature*, **475**(7357): 493−496.

Li H, Handsaker B, Wysoker A, Fennell T, Ruan J, Homer N, et al. 2009. The sequence alignment/map format and SAMtools. *Bioinformatics*, **25**(16): 2078−2079.

Li YL, Xue DX, Zhang BD, Liu JX. 2019. Population genomic signatures of genetic structure and environmental selection in the catadromous roughskin sculpin *Trachidermus fasciatus*. *Genome Biology and Evolution*, **11**(7): 1751−1764.

Li ZY, Yu L, Zhang YZ, Gao J, Zhang PZ, Wan B, et al. 2001. Identification of human, mouse and rat *PPP1R14A*, protein phosphatase-1 inhibitor subunit 14A, & mapping human *PPP1R14A* to chromosome 19q13.13-q13.2. *Molecular Biology Reports*, **28**(2): 91−101.

Liu BJ, Zhang BD, Xue DX, Gao TX, Liu JX. 2016. Population structure and adaptive divergence in a high gene flow marine fish: The small yellow croaker (*Larimichthys polyactis*). *PLoS One*, **11**(4): e0154020.

Liu LL, Zhu H, Yan YC, Wang XW, Zhang R, Zhu JY. 2018. Research progress of cold tolerance mechanism and functional genes in fish. *Biotechnology Bulletin*, **34**(8): 50−57. (in Chinese)

Maksimov EG, Mironov KS, Trofimova MS, Nechaeva NL, Todorenko DA, Klementiev KE, et al. 2017. Membrane fluidity controls redox-regulated cold stress responses in cyanobacteria. *Photosynthesis Research*, **133**(1–3): 215−223.

Masutani C, Kusumoto R, Yamada A, Dohmae N, Yokoi M, Yuasa M, et al. 1999. The *XPV* (xeroderma pigmentosum variant) gene encodes human DNA polymerase η. *Nature*, **399**(6737): 700−704.

McKay RJ. 1992. Sillaginid fishes of the world (Family Sillaginidae). Rome: Food and Agriculture Organization of the United Nations.

Oka OBV, Pringle MA, Schopp IM, Braakman I, Bulleid NJ. 2013. ERdj5 is the ER reductase that catalyzes the removal of non-native disulfides and correct folding of the LDL receptor. *Molecular Cell*, **50**(6): 793−804.

Oozeki Y, Hwang PP, Hirano R. 1992. Larval development of the Japanese whiting, *Sillago japonica*. *Japanese Journal of Ichthyology*, **39**(1): 59−66.

Oshima S, Nakamura T, Namiki S, Okada E, Tsuchiya K, Okamoto R, et al. 2004. Interferon Regulatory Factor 1 (IRF-1) and IRF-2 distinctively up-regulate gene expression and production of interleukin-7 in human intestinal epithelial cells. *Molecular and Cellular Biology*, **24**(14): 6298−6310.

Phillips SJ, Anderson RP, Schapire RE. 2006. Maximum entropy modeling of species geographic distributions. *Ecological Modelling*, **190**(3–4): 231−259.

Pickrell JK, Pritchard JK. 2012. Inference of population splits and mixtures from genome-wide allele frequency data. *PLoS Genetics*, **8**(11): e1002967.

Purcell S, Neale B, Todd-Brown K, Thomas L, Ferreira MAR, Bender D, et al. 2007. PLINK: a tool set for whole-genome association and population-based linkage analyses. *The American Journal of Human Genetics*, **81**(3): 559−575.

Rouhiainen A, Zhao X, Vanttola P, Qian K, Kulesskiy E, Kuja-Panula J, et al. 2016. HMGB4 is expressed by neuronal cells and affects the expression of genes involved in neural differentiation. *Scientific Reports*, **6**: 32960.

Russell NJ, Nichols DS. 1999. Polyunsaturated fatty acids in marine bacteria-a dogma rewritten. *Microbiology*, **145**(4): 767−779.

Schluter D, McPeek MA. 2000. Ecological character displacement in adaptive radiation. *The American Naturalist*, **156**(S4): S4−S16.

Skelly DK, Joseph LN, Possingham HP, Freidenburg LK, Farrugia TJ, Kinnison MT, et al. 2007. Evolutionary responses to climate change. *Conservation Biology*, **21**(5): 1353−1355.

Spivakov M, Auer TO, Peravali R, Dunham I, Dolle D, Fujiyama A, et al. 2014. Genomic and phenotypic characterization of a wild medaka population: towards the establishment of an isogenic population genetic resource in fish. *G3: Genes-Genomes-Genetics*, **4**(3): 433−445.

van Meer G, Voelker DR, Feigenson GW. 2008. Membrane lipids: Where they are and how they behave. *Nature Reviews Molecular Cell Biology*, **9**(2): 112−124.

Wang J, Xue DX, Zhang BD, Li YL, Liu BJ, Liu JX. 2016. Genome-wide SNP discovery, genotyping and their preliminary applications for population genetic inference in spotted sea bass (*Lateolabrax maculatus*). *PLoS One*, **11**(6): e0157809.

Wang K, Li MY, Hakonarson H. 2010. ANNOVAR: functional annotation of genetic variants from high-throughput sequencing data. *Nucleic Acids Research*, **38**(16): e164.

White CR, Alton LA, Frappell PB. 2012. Metabolic cold adaptation in fishes occurs at the level of whole animal, mitochondria and enzyme. *Proceedings of the Royal Society B: Biological Sciences*, **279**(1734): 1740−1747.

Wu X, Huang W, Prasad PD, Seth P, Rajan DP, Leibach FH, et al. 1999. Functional characteristics and tissue distribution pattern of organic cation transporter 2 (OCTN2), an organic cation/carnitine transporter. *Journal of Pharmacology and Experimental Therapeutics*, **290**(3): 1482−1492.

Xu SY, Song N, Zhao LL, Cai SS, Han ZQ, Gao TX. 2017. Genomic evidence for local adaptation in the ovoviviparous marine fish *Sebastiscus marmoratus* with a background of population homogeneity. *Scientific Reports*, **7**(1): 1562.

Xu SY, Yanagimoto T, Song N, Cai SS, Gao TX, Zhang XM. 2019. Population genomics reveals possible genetic evidence for parallel evolution of *Sebastiscus marmoratus* in the northwestern Pacific Ocean. *Open Biology*, **9**: 190028.

Xue TQ, Du N, Gao TX. 2010. Phylogenetic relationships of 4 Sillaginidae species based on partial sequences of COI and cytochrome *b* gene. *Journal of Ocean University China*, **40**(S1): 91−98. (in Chinese)

Yamada K, Ono M, Perkins ND, Rocha S, Lamond AI. 2013. Identification and functional characterization of FMN2, a regulator of the cyclin-dependent kinase inhibitor p21. *Molecular Cell*, **49**(5): 922−933.

Yamamoto T, Davis CG, Brown MS, Schneider WJ, Casey ML, Goldstein JL, et al. 1984. The human LDL receptor: a cysteine-rich protein with multiple Alu sequences in its mRNA. *Cell*, **39**(1): 27−38.

Yang J, Lee SH, Goddard ME, Visscher PM. 2011. GCTA: a tool for genome-wide complex trait analysis. *The American Journal of Human Genetics*, **88**(1): 76−82.

Yang TY, Gao TX, Meng W, Jiang YL. 2020. Genome-wide population structure and genetic diversity of Japanese whiting (*Sillago japonica*) inferred from genotyping-by-sequencing (GBS): Implications for fisheries management. *Fisheries Research*, **225**: 105501.

Zhang ZX, Xu SY, Capinha C, Weterings R, Gao TX. 2019. Using species distribution model to predict the impact of climate change on the potential distribution of Japanese whiting *Sillago japonica*. *Ecological Indicators*, **104**: 333−340.